JACS
JOURNAL OF THE AMERICAN CHEMICAL SOCIETY

Communication

pubs.acs.org/JACS

Effects of Additives on the Morphology of Solution Phase Aggregates Formed by Active Layer Components of High-Efficiency Organic Solar Cells

Sylvia J. Lou,[†,‡] Jodi M. Szarko,[†,‡] Tao Xu,[§] Luping Yu,*[,‡,§] Tobin J. Marks,*[,†,‡] and Lin X. Chen*[,†,‡,∥]

[†]Department of Chemistry, Northwestern University, 2145 Sheridan Road, Evanston, Illinois 60208, United States

[‡]The Argonne-Northwestern Solar Energy Research (ANSER) Center, Northwestern University, Evanston, Illinois 60208, United States

[§]Department of Chemistry and James Franck Institute, The University of Chicago, 929 East 57th Street, Chicago, Illinois 60637, United States

[∥]Chemical Sciences and Engineering Division, Argonne National Laboratory, 9700 South Cass Avenue, Argonne, Illinois 60439, United States

Supporting Information

ABSTRACT: Processing additives are used in organic photovoltaic systems to optimize the active layer film morphology. However, the actual mechanism is not well understood. Using X-ray scattering techniques, we analyze the effects of an additive diiodooctane (DIO) on the aggregation of a high-efficiency donor polymer **PTB7** and an acceptor molecule **$PC_{71}BM$** under solar cell processing conditions. We conclude that DIO selectively dissolves **$PC_{71}BM$** aggregates, allowing their intercalation into **PTB7** domains, thereby optimizing both the domain size and the **PTB7**−**$PC_{71}BM$** interface.

Increasing worldwide energy demands and environmental concerns about the impact of fossil fuel combustion have stimulated the quest for alternative energy sources. Bulk heterojunction (BHJ) organic photovoltaic (OPV) cells[1] are promising devices for alternative energy sources because they are composed of earth-abundant materials that are solution-processable and, therefore, cost-effective for large scale manufacture. Large scale implementation is currently limited by power conversion efficiencies (PCEs) of ∼7.5%[2] while >10% is highly desirable for commercial viability.[3] One factor constraining BHJ device PCEs is the morphology of the interpenetrating networks of donor and acceptor materials in the photoactive layer. To achieve high PCEs, the network must have multiple interfaces for efficient charge separation and long percolation pathways for efficient charge transfer, requiring an ideal BHJ donor/acceptor domain length scale of ≤10 nm.[4] Many largely empirical methods have been applied to achieve such morphologies, including postproduction annealing,[5] solvent annealing,[6] and the introduction of processing additives.[7]

OPV processing additives offer an attraction over annealing processes in that they do not require an additional fabrication step. Two general guidelines for additive design are as follows: (1) the boiling point must be significantly greater than that of the processing solvent to maximize the interaction time between the additive and the active layer components during thin film formation, and (2) one active layer component must be significantly more soluble in the additive than the other component.[7a] Recent promising additives fulfilling these guidelines include alkanedithiols, for which fullerene acceptor solubility and the resulting BHJ film morphologies have been characterized,[8] and di(X)octanes, where X is a small, polarizable group such as a halogen.[9] For BHJ systems containing donor polymers such as **PTB7**,[2] **PCPDTBT**,[9] and others,[10] 1,8-diiodooctane (DIO) affords the largest PCE enhancements observed to date.

The high-PCE donor polymer **PTB7**, composed of alternating thieno[3,4-*b*]thiophene and benzodithiophene units, affords a PCE of 7.4% when combined with the fullerene acceptor, [6,6]-phenyl-C_{71}-butyric acid methyl ester (**$PC_{71}BM$**; Chart 1).[2] The large PCE is attributed to both the low **PTB7** band gap, affording efficient capture of solar photons, and an ideal film morphology with domain sizes of ∼10 nm,[2] with **$PC_{71}BM$** molecules intercalating into the **PTB7** network.[11] Note that this efficacious morphology is only achieved by DIO addition, which increases the PCE by 33%.[2] While several studies reveal that processing additives promote more favorable BHJ morphologies,[12] little is understood about the microstructural evolution occurring in the transformation from solution-phase BHJ precursors to thin photoactive films.[8] In

Chart 1. Structures of Active Layer Components

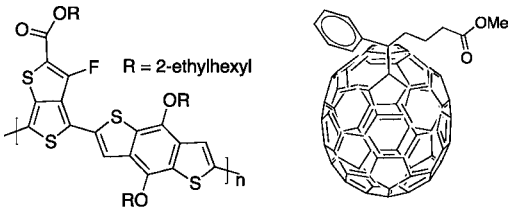

PTB7 $PC_{71}BM$

Received: September 10, 2011
Published: November 29, 2011

   dx.doi.org/10.1021/ja2085564 | *J. Am. Chem.Soc.* 2011, 133, 20661−20663

this small-angle X-ray scattering (SAXS) investigation on active layer **PTB7:PC$_{71}$BM** solutions, we find that these species are heavily aggregated and that DIO significantly affects the level of aggregation. A mechanism for thin BHJ film formation is hence proposed based on our results.

BHJ solution characterization was carried out by transmission SAXS at Beamline 5ID at the Advanced Photon Source (APS) of Argonne National Laboratory. Results are presented in terms of the reciprocal space variable Q which is approximately related to the d-spacing by $Q = 2\pi/d$. The experimental Q range ($0.01\ \text{Å}^{-1} < Q < 0.8\ \text{Å}^{-1}$) corresponds to $8\ \text{Å} < d < 628\ \text{Å}$. The scattering profiles were fit using Modeling I, Standard Models developed by J. Ilavsky for Igor Pro[13] based on the standard small angle scattering equation,

$$I(Q) = |\Delta\rho|^2 \int_0^\infty |F(Q, r)|^2 V(r)^2 N P(r) dr \quad (1)$$

where $I(Q)$ is intensity, $\Delta\rho$ the difference in electron density between the scattering particle and the surrounding medium, $F(Q,r)$ the form factor, $V(r)$ the particle volume, N the total number of particles that scatter, and $P(r)$ the probability of a scattering particle with radius r. For all systems, we assume spherical aggregates and fit experimental $I(Q)$ as a function of Q assuming either two or three log-normal distributions of aggregate size, allowing the mean size, aggregate volume, and distribution widths to vary. This fitting yields an approximate aggregate size and allows comparison of relative aggregation patterns rather than determination of absolute aggregate size. It is also important to note that this fitting will give the minimum size and a range rather than an absolute size.

To mimic BHJ cell fabrication conditions, the concentrations of the active layer components used were the same as those for optimized devices. Both single component **PTB7** and **PC$_{71}$BM** solutions as well as mixed **PTB7:PC$_{71}$BM** solutions (1:1.5 w/w) in chlorobenzene (CB) were studied either with the standard concentration of 3% v/v DIO or without DIO. The **PTB7** and **PC$_{71}$BM** concentrations were 10 and 15 mg/mL, respectively.

PTB7 aggregation in CB solutions with and without DIO were first investigated. The SAXS results reveal a double peak structure, suggesting multiple aggregate dimensions from multiple sizes of spherical aggregates or a nonspherical aggregate shape. When the scattering profile is fit assuming spheroidal aggregates, the mean radii of the peak distributions are 34.2 ± 0.4 and <8 Å within the limits of the experiment (Figure 1a, red trace). Since the second value is too small to attribute to aggregation, we suggest it corresponds to an intra-aggregate distance, such as $\pi-\pi$ stacking of the polymer backbone[1,2] within an aggregate. The **PTB7** aggregate radius is 34.2 Å, and this large size likely reflects the high **PTB7** concentration and low **PTB7** solubility. When DIO is added to the CB solution, the **PTB7** scattering signals have very little changes (Figure 1a), and the data fitting results in a slightly larger aggregate radius of 36.7 ± 0.8 Å with a similar small intra-aggregate distance of <8 Å. Hence, upon DIO addition, there is a small increase in the overall aggregate size.

Next, the effects of DIO on **PC$_{71}$BM** aggregation were investigated. The single peak in the scattering profile and the spheroidal **PC$_{71}$BM** shape suggest that **PC$_{71}$BM** forms spheroidal aggregates (Figure 1b). Using the aforementioned fitting procedure, we find that the mean radius of the aggregates is 11.5 ± 0.5 Å without DIO and <8 (fit radius of 5.7 ± 1.1) Å with DIO. In addition, the signal intensity is significantly lower

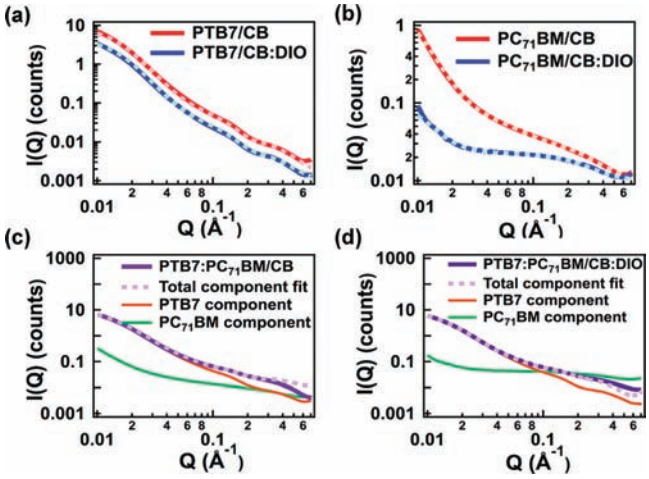

Figure 1. Experimental scattering profiles of active layer solutions (solid lines) and fits (dotted lines), comparing aggregation in CB and CB:DIO solutions of (a) **PTB7** (offset) and (b) **PC$_{71}$BM**, and two-component fits of **PTB7:PC$_{71}$BM** in (c) CB and (d) CB:DIO.

for the **PC$_{71}$BM** species in the CB:DIO solution, suggesting that there are fewer aggregates. While DIO molecules cause only slight changes in the size of the **PTB7** aggregates in solution, they selectively and completely dissolve the **PC$_{71}$BM** aggregates.

We next confirmed that the aggregation patterns in the single component solutions are the same as those in the blend solution by two methods. The first was a component fit in which the scattering intensity contributions of the **PTB7** and **PC$_{71}$BM** aggregates are separated by fitting the blend solution scattering trace $B(Q)$ with the traces of the single component solutions,

$$B(Q) = k_0 P(Q) + k_1 C(Q) + k_2 \quad (2)$$

where $B(Q)$ is the scattering profile of the blend solution, $P(Q)$ the scattering profile of the **PTB7** solution, $C(Q)$ the scattering profile of the **PC$_{71}$BM** solution, and k_0, k_1, and k_2 are fitting coefficients that describe the relative contributions of $P(Q)$ and $C(Q)$ to $B(Q)$. For the CB solutions, we find $k_0 = 0.904 \pm 0.001$, $k_1 = 0.363 \pm 0.007$, and $k_2 = 0.004 \pm 0.002$ indicating that the blend solution scattering has 71% **PTB7** character, meaning that the **PTB7** aggregates display increased scattering intensity compared to **PC$_{71}$BM** (Figure 1c). Increased scattering intensity can be related to a higher electron density, arguing that the strong **PTB7** scattering is due in part to the higher **PTB7** aggregate electron density versus the **PC$_{71}$BM** aggregates. For the CB:DIO solutions (Figure 1d), $k_0 = 0.861 \pm 0.001$, $k_1 = 1.894 \pm 0.093$, and $k_2 = -0.019 \pm 0.002$, suggesting that **PC$_{71}$BM** now scatters more strongly than the **PTB7** aggregates. Since there is very little change in the aggregation of **PTB7**, its electron density remains the same in both solutions. However, the **PC$_{71}$BM** electron density increases when DIO is added to the CB solution. This increase is due to a change in the unit volume electron density of the **PC$_{71}$BM** aggregates rather than a change in the average electron density over the entire solution. The electron density of a single molecule of **PC$_{71}$BM** in the CB:DIO solution may be higher than the electron density of a cluster of **PC$_{71}$BM** molecules in the CB solution, and therefore, the **PC$_{71}$BM** molecule will have a stronger scattering signal than the **PC$_{71}$BM** aggregate. Because of the large **PTB7** component in

dx.doi.org/10.1021/ja2085564 | J. Am. Chem.Soc. 2011, 133, 20661–20663

the blend scattering profiles, the **PTB7** scattering profile was next subtracted from that of the blend to determine the **$PC_{71}BM$** aggregate size. It is found that **PTB7** addition to the **$PC_{71}BM$** solution has little effect on the **$PC_{71}BM$** aggregate size (see Supporting Information).

DIO is an effective additive in this BHJ OPV system since it fulfills the requirement of a high boiling point and selective **$PC_{71}BM$** dissolution. Without DIO, the **$PC_{71}BM$** aggregates are large which hinders **$PC_{71}BM$** intercalation into the **PTB7** network during film formation, so that large, segregated domains form (Figure 2a). However, on DIO addition, the

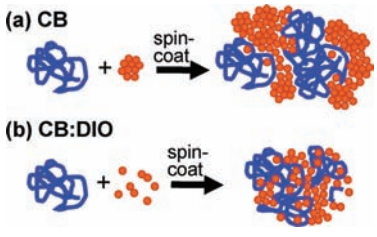

Figure 2. Schematic of **PTB7** and **$PC_{71}BM$** aggregation in (a) CB and (b) CB:DIO, and the resulting film morphology.

$PC_{71}BM$ aggregates dissolve (Figure 2b). This facilitates integration of the **$PC_{71}BM$** molecules into the **PTB7** aggregates. Furthermore, because **$PC_{71}BM$** is selectively dissolved in DIO and DIO is relatively nonvolatile, there is sufficient time for the **$PC_{71}BM$** molecules to integrate into the **PTB7** aggregates, resulting in a greater donor–acceptor interface density and smaller domains.

Using solution phase SAXS we have shown that DIO addition to a CB solution completely dissolves the **$PC_{71}BM$** aggregates, promoting formation of smaller domains and greater donor–acceptor interpenetration within the film. A possible explanation is that the iodine atom bears a partial negative charge and **$PC_{71}BM$** is electrodeficient, which may be the reason for their relatively strong interactions with each other and the enhanced solubility of **$PC_{71}BM$** in the presence of DIO. A deeper understanding of the mechanism of film formation will assist in the selection of ideal processing additives for future BHJ solar cell systems.

■ ASSOCIATED CONTENT

Ⓢ Supporting Information

Experimental details, fits of the blend solution and the $PC_{71}BM$ component in blend solutions. This material is available free of charge via the Internet at http://pubs.acs.org.

■ AUTHOR INFORMATION

Corresponding Author

l-chen@northwestern.edu; t-marks@northwestern.edu; lupingyu@chicago.edu

■ ACKNOWLEDGMENTS

This material is based upon work supported as part of the ANSER Center, an Energy Frontier Research Center funded by the U.S. Department of Energy, Office of Science, Office of Basic Energy Sciences under Award Number DE-SC0001059. L.Y. and T.X. thank the National Science Foundation (NSF DMR-1004195), the National Science Foundation-Materials Research Science and Engineering Center at University of Chicago, and the Air Force Office of Scientific Research. A portion of the equipment and laboratory setting is supported by the Division of Chemical Sciences, Office of Basic Energy Sciences, the U.S. Department of Energy under Contract DE-AC02-06CH11357 (for L.X.C.). Use of the Advanced Photon Source, an Office of Science User Facility operated for the U.S. Department of Energy (DOE) Office of Science by Argonne National Laboratory, was supported by the U.S. DOE under Contract No. DE-AC02-06CH11357.

■ REFERENCES

(1) (a) Servaites, J. D.; Ratner, M. A.; Marks, T. J. *Energ. Environ. Sci.* **2011**, *4*, 4410–4422, and references therein. (b) Service, R. F. *Science* **2011**, *332*, 293 and references therein. (c) Yu, G.; Gao, J.; Hummelen, J. C.; Wudl, F.; Heeger, A. J. *Science* **1995**, *270* (5243), 1789–1791.

(2) (a) Szarko, J. M.; Guo, J.; Liang, Y.; Lee, B.; Rolczynski, B. S.; Strzalka, J.; Xu, T.; Loser, S.; Marks, T. J.; Yu, L; Chen, L. X. *Adv. Mater.* **2010**, *22*, 5468–5472. (b) Liang, Y.; Xu, Z.; Xia, J. B.; Tsai, S. T.; Wu, Y.; Li, G.; Ray, C.; Yu, L. P. *Adv. Mater.* **2010**, *22* (20), E135–E138.

(3) Dennler, G.; Brabec, C. J. Socio-Economic Impact of Low-Cost PV Technologies. *Organic Photovoltaics*; Wiley-VCH Verlag GmbH & Co. KGaA: 2009; pp 531–566.

(4) (a) Dennler, G.; Scharber, M. C.; Brabec, C. J. *Adv. Mater.* **2009**, *21* (13), 1323–1338. (b) McGehee, M. D.; Scully, S. R. *J. Appl. Phys.* **2006**, *100*, 034907.

(5) (a) Erb, T.; Zhokhavets, U.; Hoppe, H.; Gobsch, G.; Al-Ibrahim, M.; Ambacher, O. *Thin Solid Films* **2006**, *511*, 483–485. (b) Wang, T.; Pearson, A. J.; Lidzey, D. G.; Jones, R. A. L. *Adv. Funct. Mater.* **2011**, *21* (8), 1383–1390. (c) Loser, S.; Bruns, C. J.; Miyauchi, H.; Ortiz, R. P.; Facchetti, A.; Stupp, S. I.; Marks, T. J. *J. Am. Chem. Soc.* **2011**, *133* (21), 8142–8145.

(6) (a) Miller, S.; Fanchini, G.; Lin, Y. Y.; Li, C.; Chen, C. W.; Su, W. F.; Chhowalla, M. *J. Mater. Chem.* **2008**, *18* (3), 306–312. (b) Li, G.; Yao, Y.; Yang, H.; Shrotriya, V.; Yang, G.; Yang, Y. *Adv. Funct. Mater.* **2007**, *17* (10), 1636–1644. (c) Chen, F. C.; Ko, C. J.; Wu, J. L.; Chen, W. C. *Sol. Energy Mater. Sol. Cells* **2010**, *94* (12), 2426–2430.

(7) (a) Pivrikas, A.; Neugebauer, H.; Sariciftci, N. S. *Sol. Energy* **2011**, *85* (6), 1226–1238. (b) Hoven, C. V.; Dang, X. D.; Coffin, R. C.; Peet, J.; Nguyen, T. Q.; Bazan, G. C. *Adv. Mater.* **2010**, *22* (8), E63–E66.

(8) Salim, T.; Wong, L. H.; Brauer, B.; Kukreja, R.; Foo, Y. L.; Bao, Z. N.; Lam, Y. M. *J. Mater. Chem.* **2011**, *21* (1), 242–250.

(9) Lee, J. K.; Ma, W. L.; Brabec, C. J.; Yuen, J.; Moon, J. S.; Kim, J. Y.; Lee, K.; Bazan, G. C.; Heeger, A. J. *J. Am. Chem. Soc.* **2008**, *130* (11), 3619–3623.

(10) Zhang, Y. G.; Li, Z.; Wakim, S.; Alem, S.; Tsang, S. W.; Lu, J. P.; Ding, J. F.; Tao, Y. *Org. Electron.* **2011**, *12* (7), 1211–1215.

(11) Guo, J. C.; Liang, Y. Y.; Szarko, J.; Lee, B.; Son, H. J.; Rolczynski, B. S.; Yu, L. P.; Chen, L. X. *J. Phys. Chem. B* **2010**, *114* (2), 742–748.

(12) Di Nuzzo, D.; Aguirre, A.; Shahid, M.; Gevaerts, V. S.; Meskers, S. C. J.; Janssen, R. A. J. *Adv. Mater.* **2010**, *22* (38), 4321–4324.

(13) Ilavsky, J. Modelling I, Standard Models. *Igor Pro 6.2*, 2007.